DOI: 10.21062/mft.2024.032 http://www.journalmt.com

Tribological Properties of 3D Printed Materials in Total Knee Endoprosthesis

Matus Varhanik (0000-0001-8108-0070)[1], Josef Sedlak (0000-0002-9819-8259)[1], Zbynek Studeny (0000-0003-3189-6738)[2], Patricia Janigova (0009-0009-8742-5370)[3], Felicita Chromjakova (0000-0002-5084-1153)[4]
[1]Department of Machining Technology, Institute of Manufacturing Technology, Faculty of Mechanical Engineering, Brno University of Technology, Technicka 2896/2, Brno 616 69, Czech Republic. E-mail: 193091@vutbr.cz, matus.varhanik@vutbr.cz, sedlak@fme.vutbr.cz
[2]Department of Mechanical Engineering, Faculty of Military Technology, University of Defence in Brno, Kounicova 65, Brno 602 00, Czech Republic. E-mail: zbynek.studeny@unob.cz
[3]Department of Biomedical Engineering, Faculty of Electrical Engineering and Communication, Brno University of Technology, Technicka 3082/12, Brno 616 00, Czech Republic. E-mail: 231027@vut.cz
[4]Tomas Bata University in Zlín, Faculty of Management and Economics, Department of Industrial Engineering and Information Systems, Mostní 5139, Zlín 760 01, Czech Republic. E-mail: chromjakova@utb.cz

The submitted paper deals with biotribological contact in total knee arthroplasty. The goal was to evaluate the influence of the metal component production technology on tribological parameters in defined environments. The reference sample was a standard available test ball made of the subject material, used in testing tribological properties by the "Ball on Pin" method. The preparation of the experiment consisted in the production of test disks from UHMWPE (Ultra High Molecural Weight Polyethylene) material and the production of a metal test component with a spherical surface. The condition of the experiment and the basis of this contribution is to compare the properties of conventionally produced metal material against 3D printing. Using the SLM method, a sample with a semi-spherical surface on a cylindrical shank was produced, which was subsequently ground and polished to reflect the characteristics of the standard supplied test ball. The last step was the production of a suitable fixture in order to fit the sample into the tribometer. The so-called dry friction of the heterogeneous Ti6Al4V–UHMWPE pair and the friction in a biological lubricating environment represented by bovine serum were evaluated. The evaluation of the contact surfaces took place using a profilometer and an electron microscope. The coefficient of friction was determined directly from the test device - tribometer.

Keywords: Biotribological properties, Friction of 3D printed materials, Ti6Al4V-UHMWPE contact

1 Introduction

The most common cause of knee joint disease is primary gonarthrosis, post-traumatic development of arthrosis, chondromalacia patella, cancer. These causes result in increased wear of the articulating surfaces of the knee joints [1, 2, 3].

Regarding the statistical data of the whole problem, it is estimated that about 15% of the global population suffers from osteoarthritis of the knee joints. The value of those affected increases with age, when we see that more than 55% of patients in the group of people older than 65 years suffer from arthrosis, and in the group of the population older than 75 years, degenerative changes of articulating joint surfaces occur in 80% of the population [3, 4].

Tests of tribological properties enable the examination of a whole range of quantities and parameters of a given tribological system. This system includes an indenter fitted with a ball or a tip and the sample to be examined. The system also includes the environment in which tribological testing takes place. The environment is defined by temperature, humidity and any lubricant additive. The testing system is completed by a machine - a tribometer, which controls the entire system. From the point of view of an objective comparison of the results, the testing is suitable to be carried out in laboratory conditions. From the point of view of evaluating tribological properties, friction and wear processes are investigated [5, 6, 7].

1.1 Tribology – theoretical analysis

As a tribological process, friction can be characterized by the loss of mechanical energy during mutual contact between two friction surfaces. A whole series of processes and changes take place in the course of spawning. The aforementioned mechanical energy is transformed into thermal energy, which worsens the tribological conditions of the functional surfaces, resulting in wear. The basic evaluation parameter of the contact pair is the coefficient of friction. This coefficient is a dimensionless quantity and expresses the ratio between the friction force Ft and the normal force Fn [5, 6, 7, 8].

$$\mu = \frac{F_t}{F_N}\ [-] \quad (1)$$

Depending on the method of mutual movement of the functional surfaces, the friction coefficient can be divided into [5, 6, 7]:

- Coefficient of sliding / shearing friction,
- Coefficient of rolling friction.

During the friction process of the contact surfaces, three basic states can occur [5, 6, 7, 8]:

- Dry friction – occurs in the case of direct contact between the surfaces of solid bodies,
- Liquid friction – occurs when solid bodies are separated by a liquid layer,
- Mixed friction – is a combination of both of the above-mentioned phenomena.

The coefficient of friction is defined by the following characteristics. The value of the coefficient of friction is directly affected by the state of the surface of the sample, its roughness and the state of the surface and the roughness of the indenter. When overcoming irregularities, there is a change in the load in the contact surface of the sample and the indenter. The value of the friction coefficient is influenced by the measurement time, temperature and the distance that the indenter must cover. Other environmental influences that can influence the measurement of the friction coefficient should be minimized by performing the experiment in laboratory conditions [5, 6, 7, 8].

Wear can be expressed as an undesirable permanent change in the quality of the surface or even the size of solid bodies. This change can occur either directly by the contact of two bodies (dry friction) or indirectly by means of an inserted medium (liquid friction). In addition to mechanical influences, other physical, chemical, radiation and other processes affect the change in surface quality.

The result of wear is the removal or displacement of particles of the mass of a rigid body from its functional surfaces. This results in a change in geometry, a change in the structure and properties of the functional surfaces, which lead to deviations from the optimal, pre-designed operating parameters. The speed of these changes depends on the mutual hardness of the contact surfaces, the method of their production and on other environmental conditions, which are defined in tribometer tests [9, 10].

1.2 Characteristics of 3D printed titanium and its alloys

Titanium and its alloys are materials used in various fields for their unique physical and mechanical properties. In the field of biotechnology, they are advantageously used for their biocompatibility and safety. On the other hand, their low tribological properties are found, which are caused by increased and unstable friction, adhesive wear and low resistance to abrasion [11] .

Implants are cyclically loaded components that come into contact with other materials of organic and inorganic origin, therefore it is important to investigate and improve their tribological properties. Several factors affect the tribological properties of the 3D printed titanium alloy, in our case Ti6Al4V. Hardness of the surface layer, microstructure, crystalline phase structure, surface roughness or porosity. These factors are influenced by the type of printing method used and heat treatment. The authors of the article [11] compared several production methods - SLM, SLM-HIP, EBM, hot-worked. The results of the study showed the lowest values of the coefficient of friction in the case of using the SLM method, and this method was also characterized by the highest hardness value of the surface layer HV1 [11].

The achieved surface roughness when using the SLM method for printing the Ti6Al4V alloy is Ra 9-12 μm, when using the EBM method, the roughness parameters Ra reach values of 25-35 μm. When using the SLM method, a martensitic microstructure is formed, whereas with the EBM method, a stable α+β lamellar microstructure occurs in the material. This affects the hardness achieved during heat treatment. In the case of the EBM method, the hardness is more stable depending on the annealing temperature. During the annealing of the material produced by the SLM method, due to the martensitic microstructure, it is possible to observe a peak increase in hardness to the value of 400 HV1, which occurs at a temperature of 600 °C [12].

With a standard titanium alloy implant, the experimentally measured hardness was 201 to 353 HV, the average microhardness of the given implant was 309 HV0.5 [13].

The environment of the human body exposes used implants to corrosion processes - oxidation. A corrosion layer of TiO2 is formed on the surface of the implant, which can worsen the tribological properties of the implants. The authors of the article [14] investigated the causality between the roughness of the implant surface and the formation of the TiO2 layer. A higher surface roughness resulted in a faster formation of the TiO2 layer, and at the same time, with a higher surface roughness, the thickness of the oxidation layer also increased [14]. On the other hand, with deteriorated surface roughness, there is faster growth and better attachment of tissues and cells. For this reason, implants are characterized by complex properties of surface roughness on individual surfaces.

2 Experiment - methodology

- Preparation / production of test metal samples - indentors.
- Production of UHMWPE samples according to the predefined geometry of the tribometer.
- Testing and evaluation of sliding properties of UHMWPE-Ti6Al4V, UHMWPE-additively produced Ti6Al4V contact - dry conditions..
- Testing and evaluation of the sliding properties of the contact UHMWPE-Ti6Al4V, UHMWPE-additively produced Ti6Al4V - conditions with lubricating fluid.
- Analysis of wear of contact surfaces (SEM).

2.1 Used devices

The machines and devices used in the course of testing the tribological properties of the selected heterogeneous material contact are listed in the table (Tab. 1).

Tab. 1 *List of used machines*

Measuring devices	Evaluation devices
Tribometer Bruker UMT-3	Electron microscope Zeiss EVO LS10
	TalySurf CLI 1000 surface texture measuring device

The most important part of the puzzle of the experiment was the measuring device, a tribometer from Bruker with the model designation UMT-3. The tribometer used allows setting the following parameters of the experiment:

- Tempering the working chamber to a temperature of 350 °C,
- Maximum selected normal force up to 200 N,
- The radius of rotation for a specific type of flat disc can be set between 15 and 30 mm.

The above-mentioned device makes it possible to evaluate the position of the indenter in the vertical axis Z. Thus, after the specified number of cycles, it is possible to evaluate the change in the position of the indenter, which indicates the degree of wear of the tested sample of the indenter. If, during the test, wear occurs mainly in the tested material, the value of the change in the position of the axis corresponds to the wear of the sample. In the event that there is also wear of the indenter, this value is unreliable, and after evaluating the trace of wear, it is necessary to use another, for example, profilometric method [9].

Using the Ball on Disc test method, it is possible to measure the coefficient of friction. The principle of measurement of the Ball on Disc method is the indentation of the indenter, the ball into the rotating test body. The ball is attached to a stationary fixture and is pressed with a constant force on the test sample, which is attached to the rolling table. In the event that the lubrication measurement option is selected, the assembly is supplemented with a cover plate with screws, through which the lubricating liquid (Fig. 1) is introduced during rotation and its flow is ensured [15].

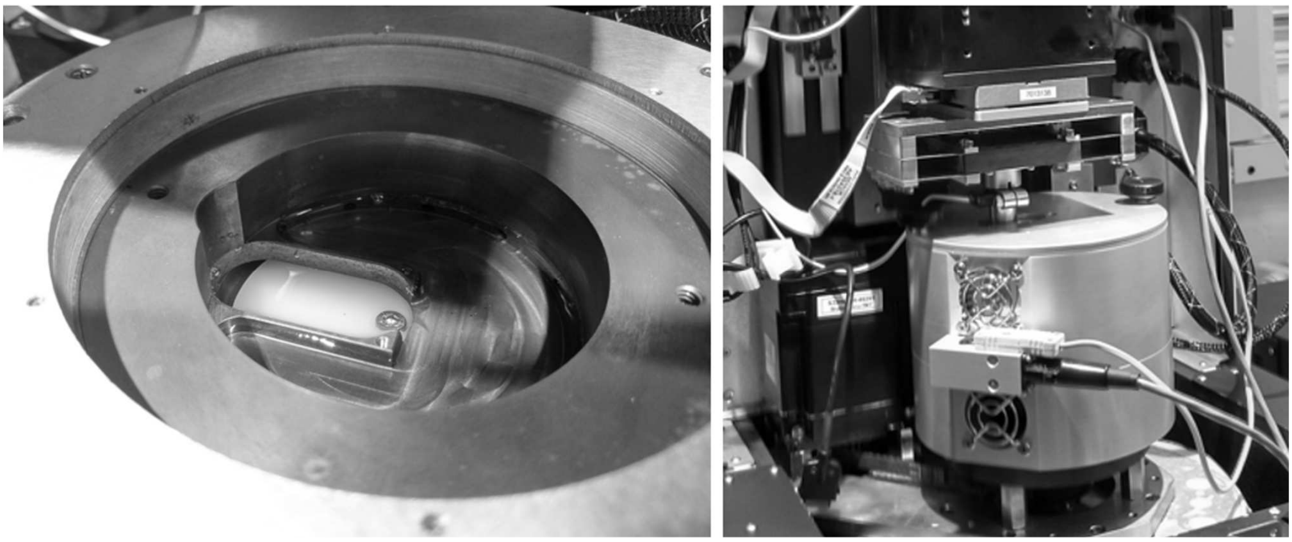

Fig. 1 *Lubricant cover (left), tribometer tempered chamber (right)*

Another instrument used was profilometric analysis. Profilometric analysis evaluates the data of the footprint, such as its width, depth of the profile and the area of the transverse profile of the footprint [16]. For statistical analysis, it is necessary to use measurements in at least six places for the evaluation.

To evaluate the wear coefficient, the key data is the footprint area. The wear coefficient is given by the relation [17]:

$$K = \frac{A_p}{F_N . \omega . t} \; [-] \qquad (2)$$

Where:

K…The wear coefficient [$mm^{-3}.N^{-1}.m^{-1}$],

Ap…The area of the wear track profile [mm^2],

FN…The normal force [N],

ω…The rotation speed of the sample [min^{-1}],

t…The measurement time [min].

The measurement of wear marks was carried out on a universal device for measuring surface texture Talysurf CLI 100 (Fig. 2), using the inductive touch method. The wear trace parameters were evaluated using the TalyMap 4.1 software. and are listed in the table (Tab. 2).

The wear trace parametersmare listed in the table (Tab. 3).

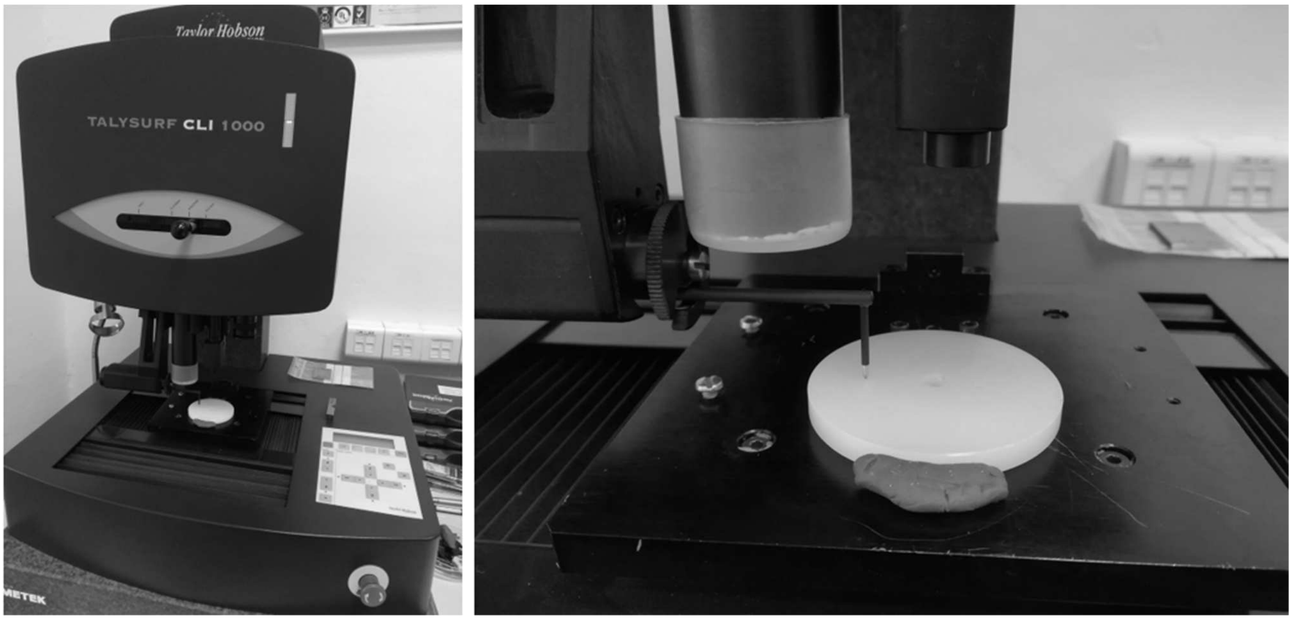

Fig. 2 *Profilometer Talysurf (right), attached sample (left)*

Tab. 2 *Parameters of measurements of wear traces*

Sensor type	Range	Resolution		Capture speed
Induction, DIA tip R2 μm	500 μm	vertical	transversely	200 μm.s-1
		10 nm	2 μm	

Tab. 3 *Conditions for measuring of wear traces*

Measured length	Data capture step	Basic length	Filtration
2 mm	3 μm	0.25 mm	Gauss – 0.25 mm

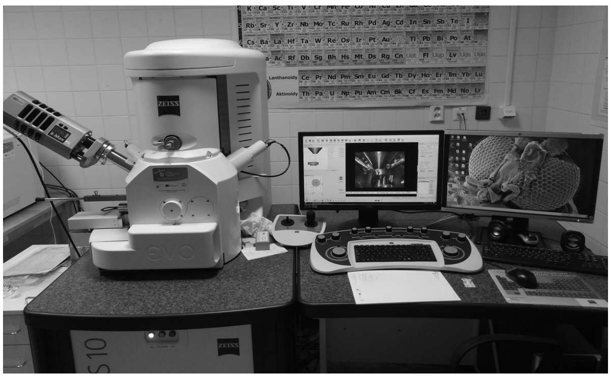

Fig. 3 *Zeiss electron microscope*

A Zeiss EVO LS10 electron microscope was used to evaluate the shape of the surface of the wear mark (Fig.3). This device was also used to scan the wear surface of the 3D printed indenter.

2.2 Experiment parameters

In the course of the experimental part, 8 tribological tests of the contact surfaces were performed. All 8 tests were subsequently repeated and processed statistically in order to minimize random measurement phenomena. The table below (Tab. 4) provides an overview of the conditions of individual measurements. All measurements were carried out at a constant temperature of 37 °C in the tempered chamber of the tribometer. The chosen temperature corresponds to the natural temperature of the knee joint of the human body. The duration of each test cycle was 1 hour.

***Tab. 4** Measuerement conditions*

Type of tribological contact	Loading force	
Ti6Al4V 3D print - UHMWPE	10 N	20 N
Ti6Al4V – UHMWPE	10 N	20 N
Ti6Al4V 3D print – UHMWPE + liquid	10 N	20 N
Ti6Al4V – UHMWPE + liquid	10 N	20 N

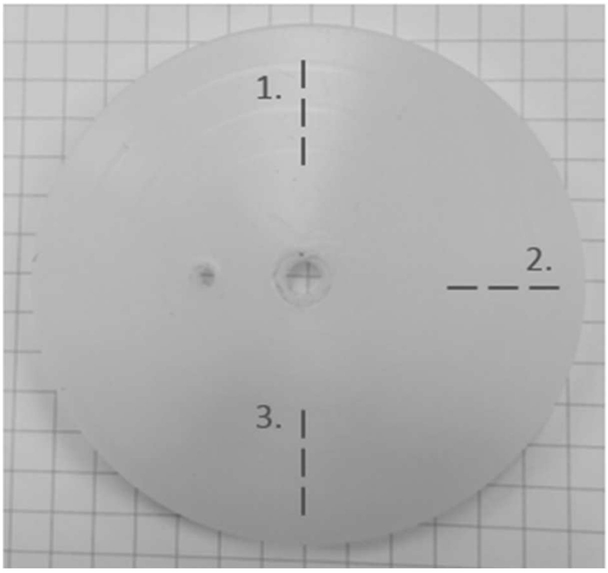

***Fig. 4** UHMWPE test plate*

***Fig. 5** Standard made indenter with holder*

The image below (Fig. 4) shows an example of a test sample (UHMWPE disk) marked with test traces, the standard supplied indenter made of Ti6Al4V material with a clamp is shown in the image (Fig. 5).

The middle trace reflects the loading force of 15 N, which served as a control value to verify the trend of the wear course of dependence on increasing load.

The indentor, manufactured using 3D printing (Fig. 6), was subsequently machined and polished to preserve the geometric and surface characteristics. Fixing the 3D printed indenter, a custom-made clamp was constructed so that the indenter could be used with a given type of tribometer (Fig. 7).

***Fig. 6** 3D printed indenter*

***Fig 7** Indenter holder with post-processing indenters*

Chemical composition of used Ti6Al4V powder is mentioned in the table (Tab. 5) below. 3D printing was carried out using SLM technology on the device TRUMPF TruPrint 1000. Used laser power was 400 W in inert argon atmosphere and step of the printer was 0.05 mm.

Tab. 5 *Chemical composition of used Ti6Al4V powder*

Element	Ti	Al	V	Fe	O	C	N	H	Y
Mass [%]	≤90	5.5 – 6.5	3.5 – 4.5	≤ 0.25	≤ 0.13	≤ 0.08	≤ 0.05	≤ 0.012	≤ 0.005

3 Results and discussion

This chapter presents the course and value of the coefficient of friction (COF) of individual contacts, which were obtained directly from the Brucker tribometer. These data were statistically processed and reflected in the graphs below (Fig. 8–11). Groups of graphs are for comparison in pairs of the same conditions with change of indenter 3D Ti6Al4V vs. Conventionally produced Ti6Al4V.

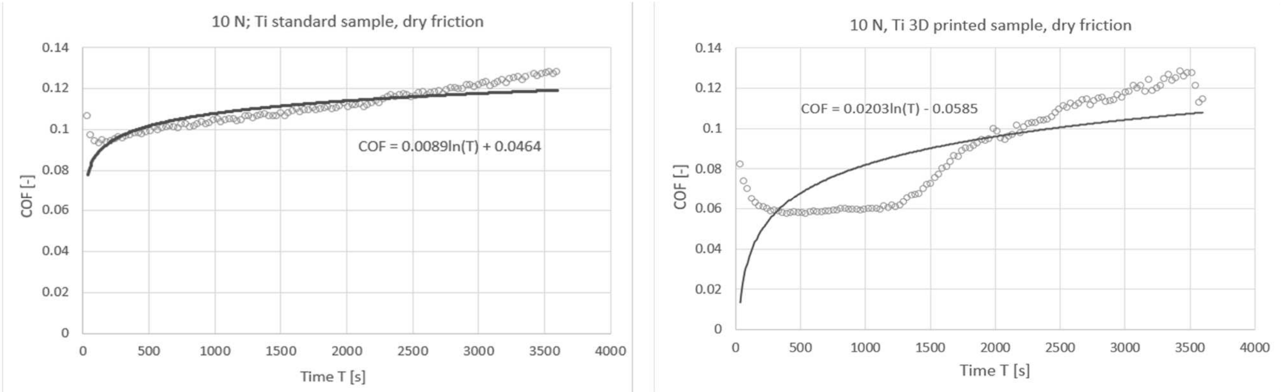

Fig. 8 *Tribological dry friction test, load 10 N*

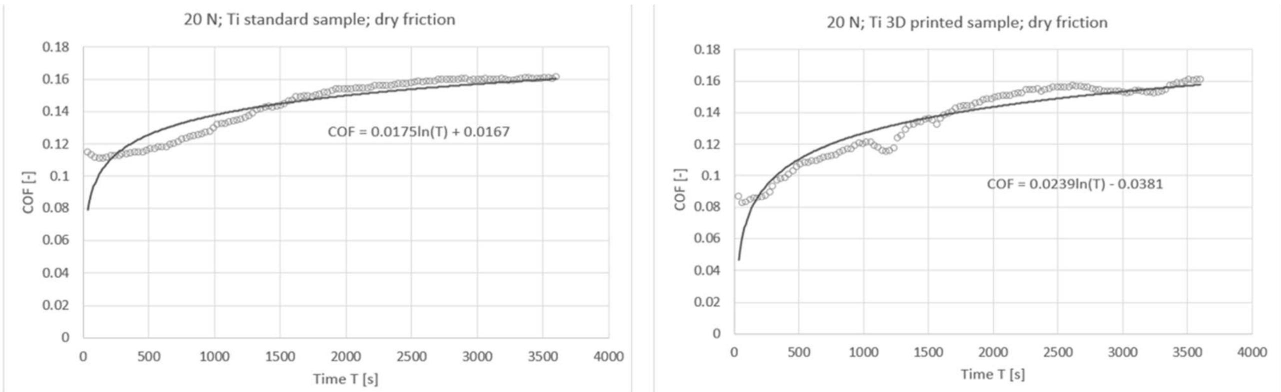

Fig. 9 *Tribological dry friction test, load 20 N*

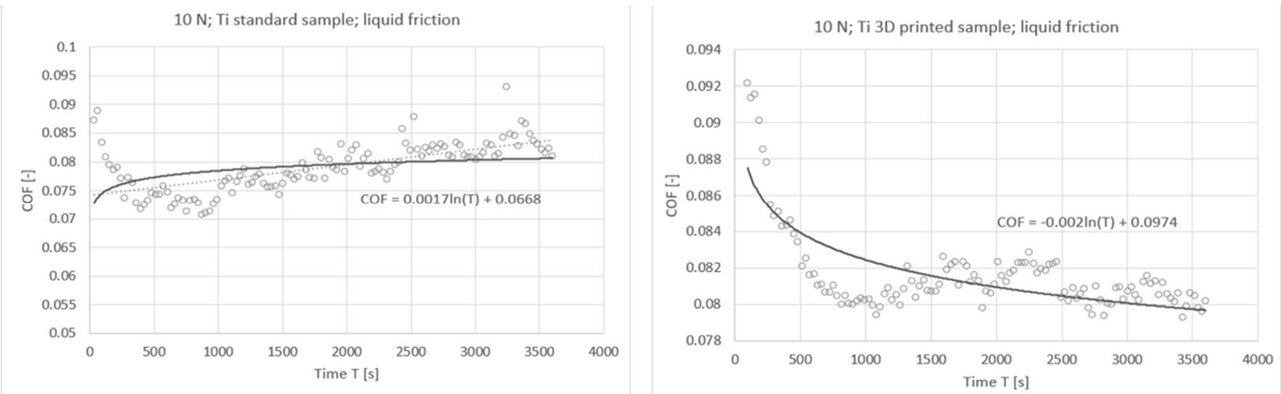

Fig. 10 *Tribological liquid friction test, load 10 N*

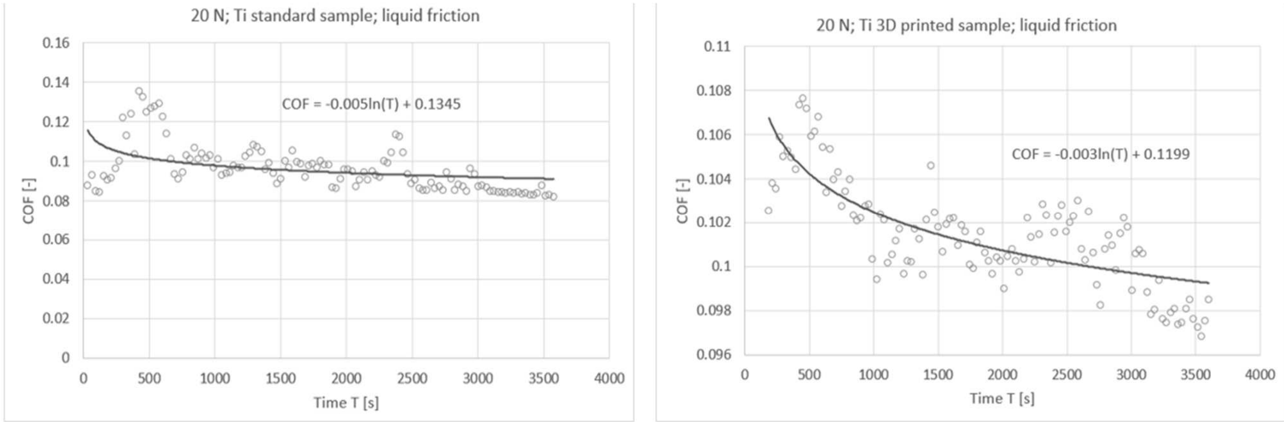

Fig. 11 *Tribological liquid friction test, load 20 N*

The data of the coefficient of friction is supplemented by the evaluation of the wear of the track, using a profilometer, which was created on a UHMWPE sample. The results of a load force of 20 N under dry friction conditions for a Ti6Al4V indenter and a 3D printed Ti6Al4V indenter in contact with a test sample are transferred to this work. These conditions for track evaluation were chosen deliberately, in order to create an environment where the most significant wear is assumed. A comprehensive evaluation of track wear is given using the measured track area (Fig. 12, 13).

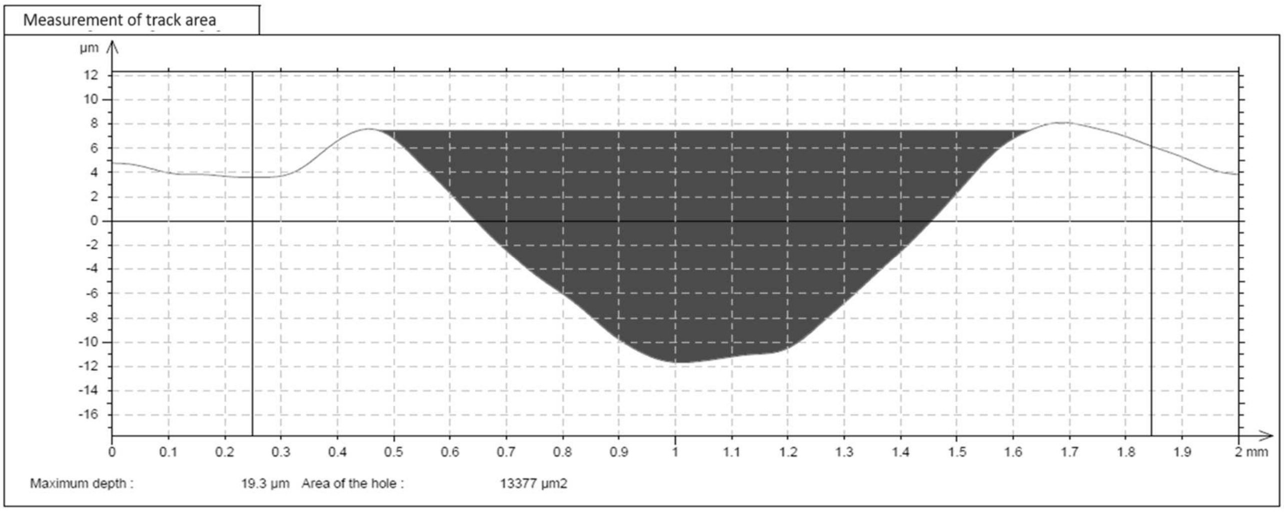

Fig. 12 *Measured footprint area for dry friction, indenter Ti standard, load 20 N*

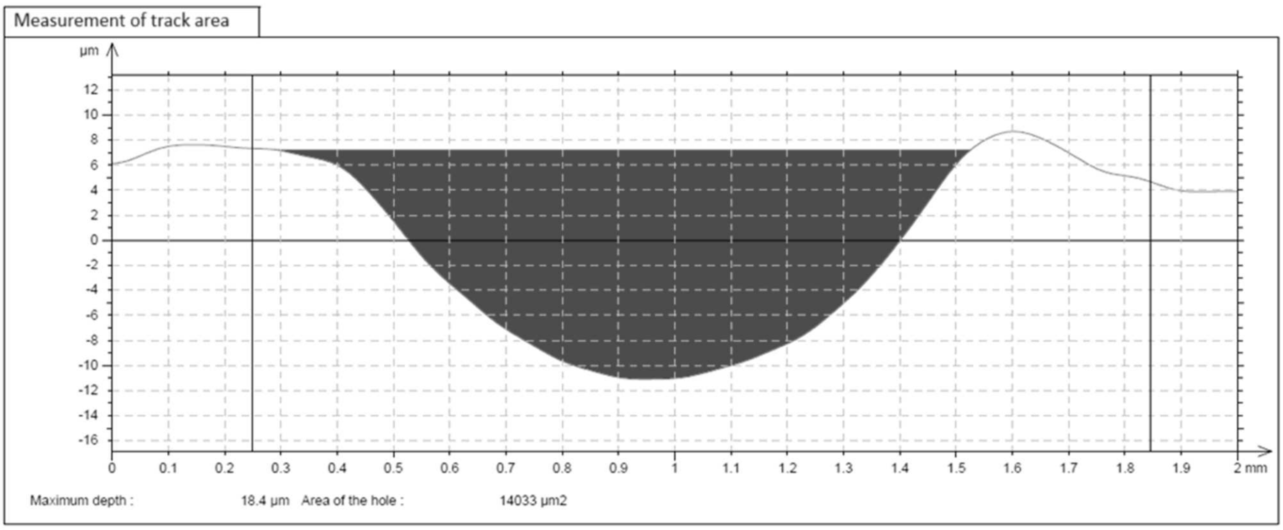

Fig. 13 *Measured footprint area for dry friction, indenter Ti 3D printing, 20 N load*

A final wear assessment was performed using an electron microscope. Thanks to this device, it is possible to monitor not only the shape and dimensions of the wear marks, but also the wear mechanisms on the surface of the marks. For clarity, the images are arranged in groups with similar input parameters. First, the dry friction conditions for a standard-made titanium alloy indenter followed by a 3D-printed indenter are shown (Fig. 14-17).

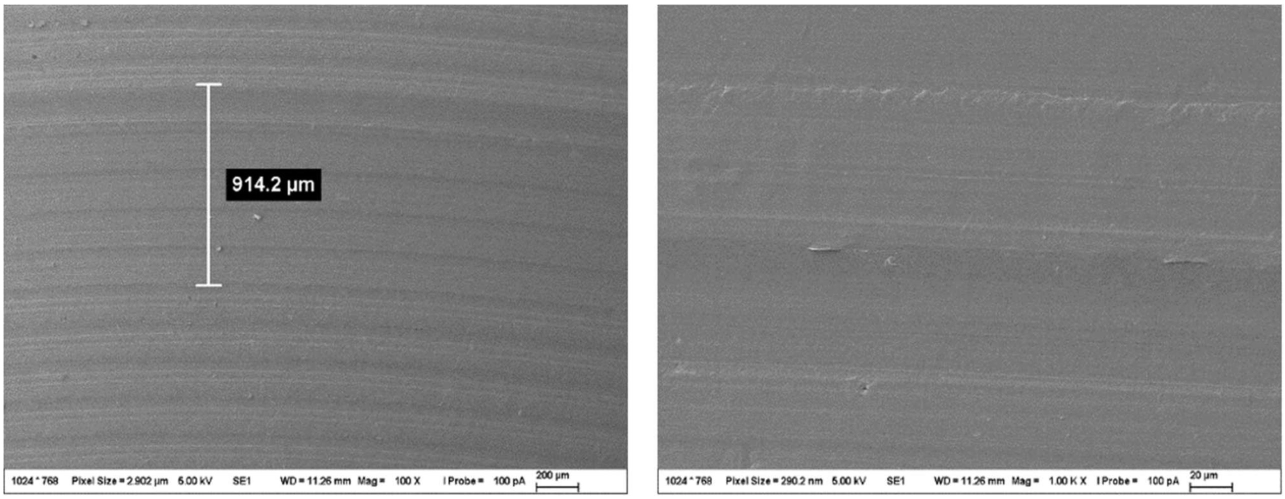

Fig. 14 *Load 10 N, dry friction (magnification 100x left, 1000x right), 3D printing Ti*

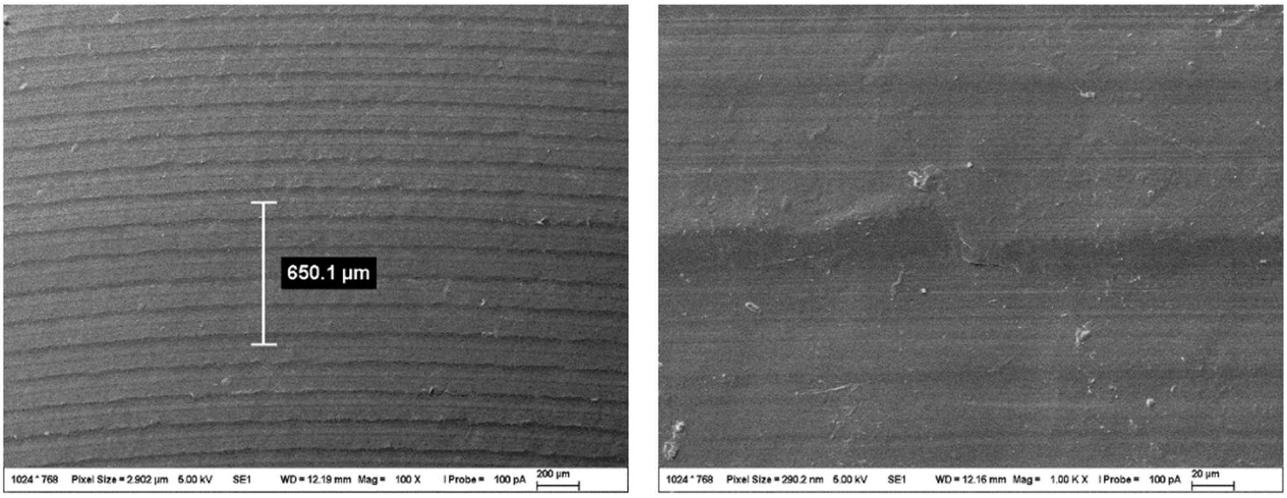

Fig. 15 *Load 10 N, dry friction (magnification 100x left, 1000x right), Ti standard*

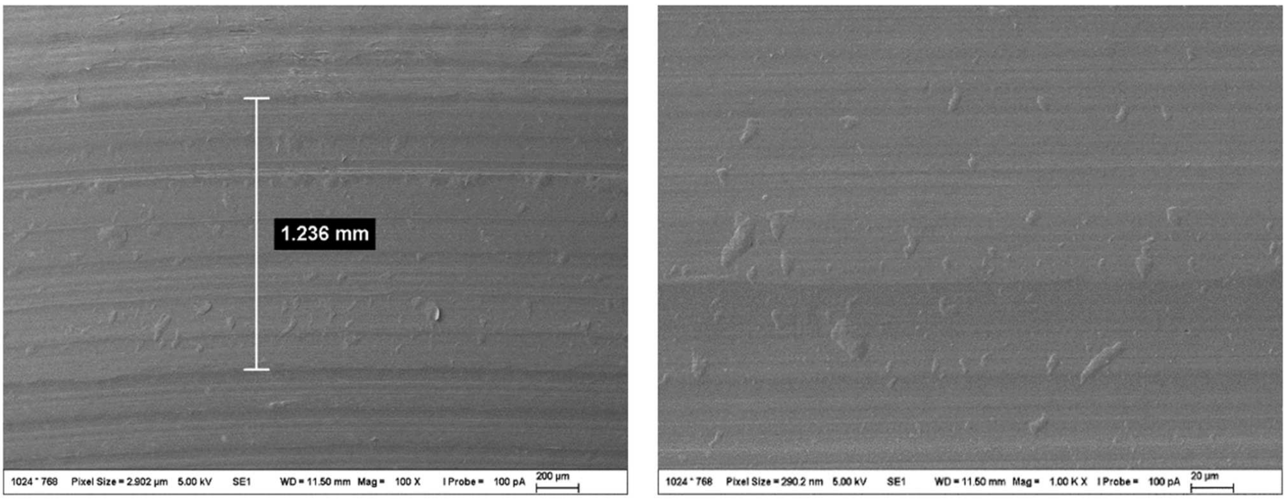

Fig. 16 *Load 20 N, dry friction (magnification 100x left, 1000x right), 3D printing Ti*

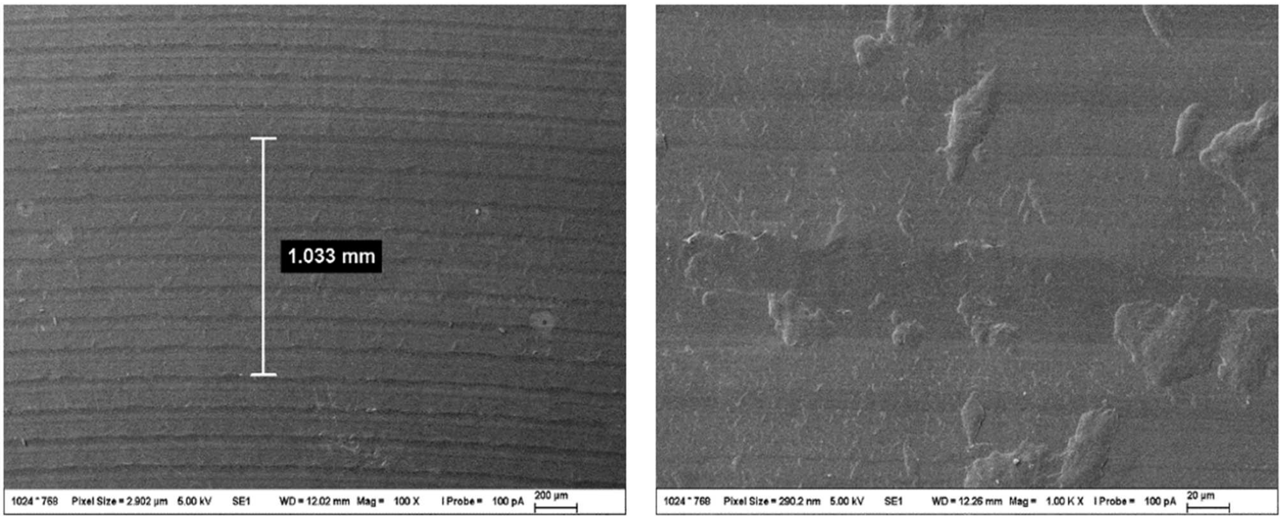

Fig. 17 *Load 20 N, dry friction (magnification 100x left, 1000x right), Ti standard*

The images below show the fluid friction conditions. The liquid, or lubricant, was represented by bovine serum diluted in proportion with distilled water. The dilution ratio is determined by the ISO 14243-3 standard (Fig. 18-21).

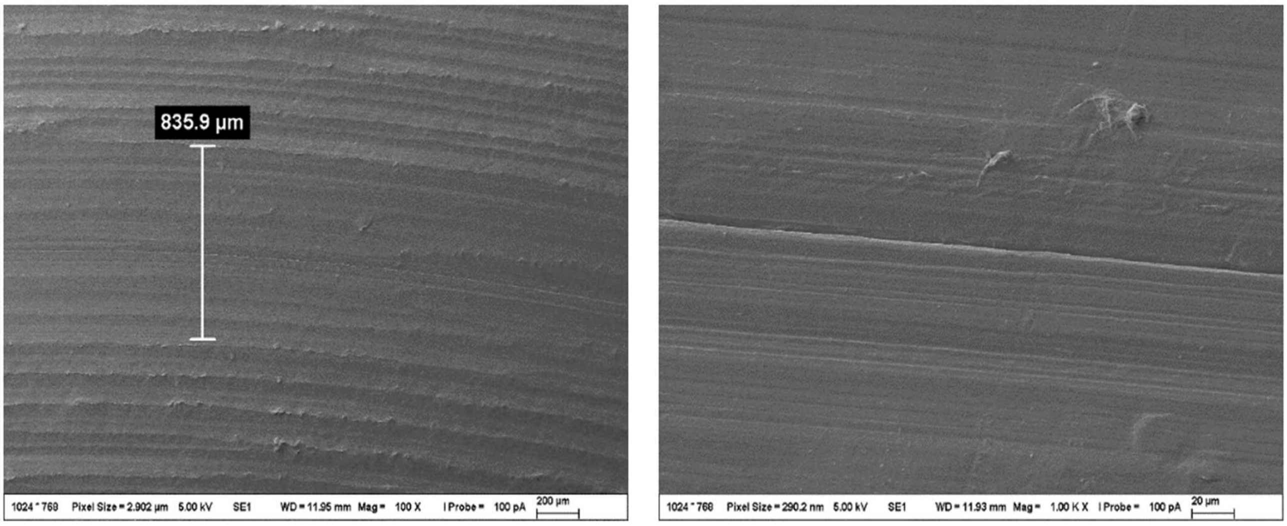

Fig. 18 *10 N load, fluid friction (magnification 100x left, 1000x right), 3D printing Ti*

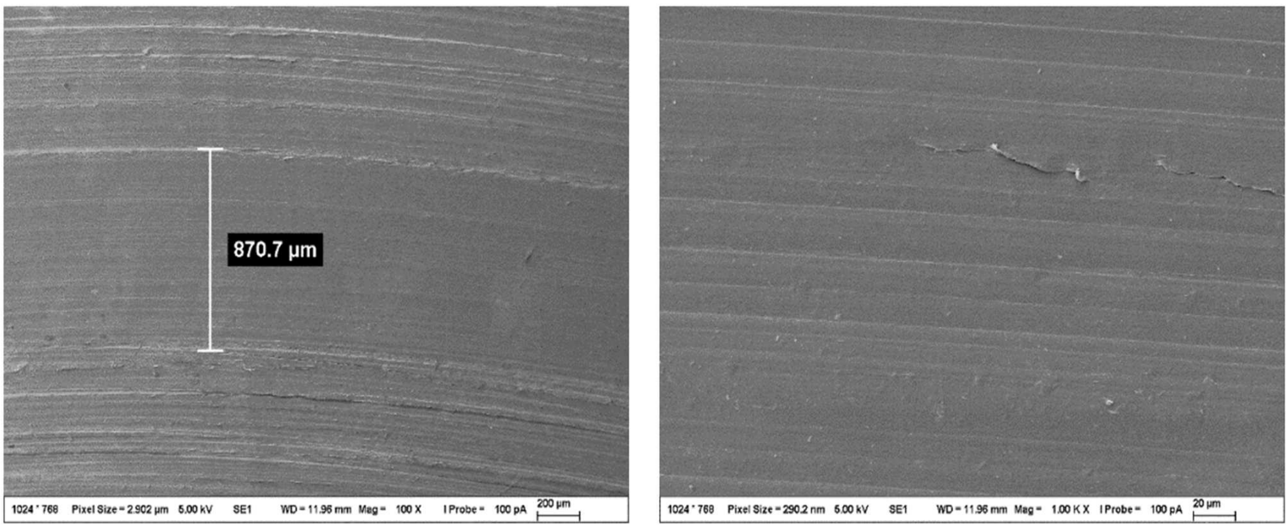

Fig. 19 *10 N load, fluid friction (magnification 100x left, 1000x right), Ti standard*

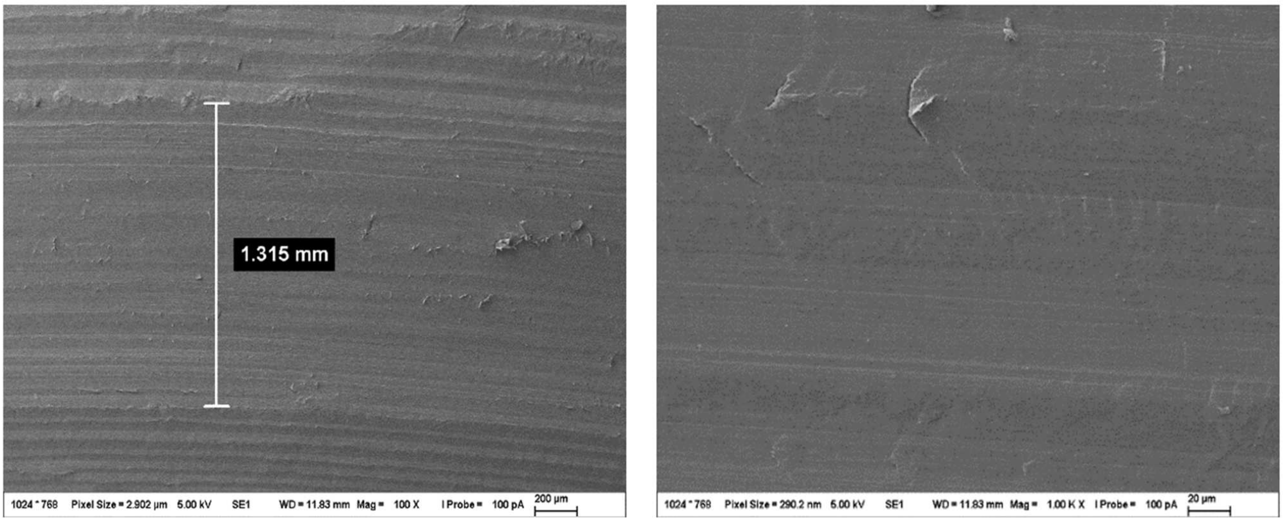

Fig. 20 *20 N load, fluid friction (magnification 100x left, 1000x right), 3D printing Ti*

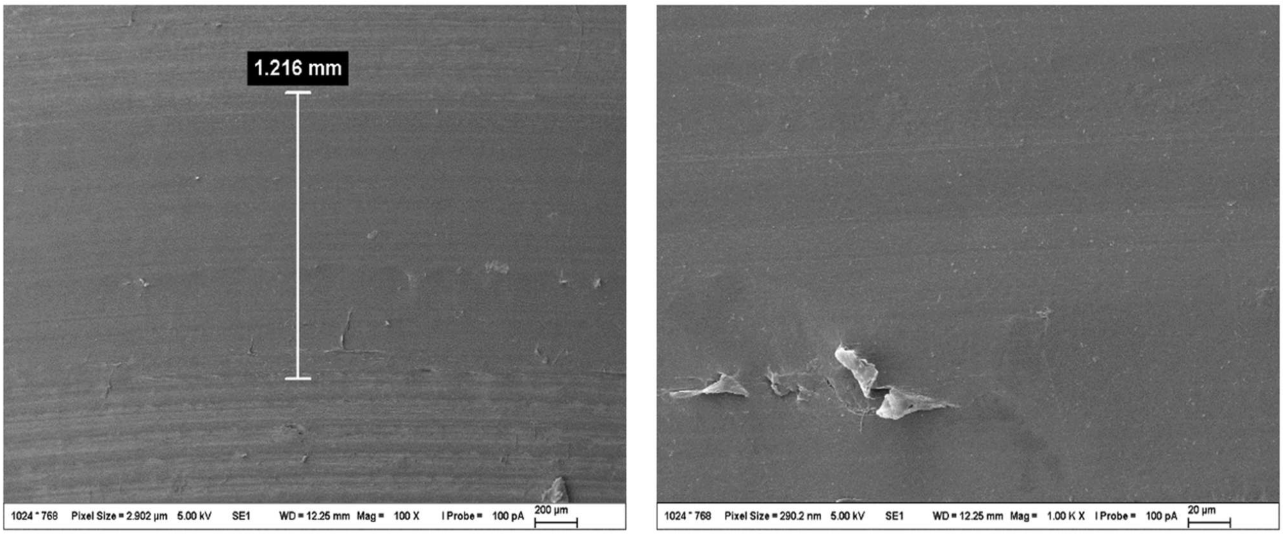

Fig. 21 *20 N load, fluid friction (magnification 100x left, 1000x right), Ti standard*

The spherical surface of the used indentors was also scanned with an electron microscope, on which the changes caused by mutual tribological contact are recorded (Fig. 22, 23).

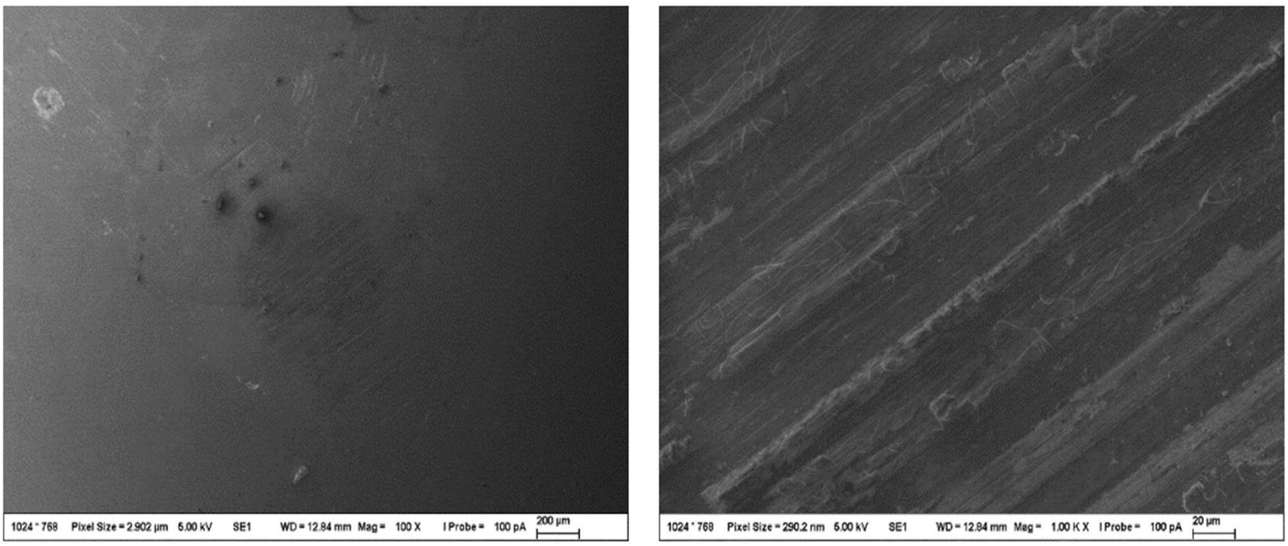

Fig. 22 *3D Ti indenter wear, magnification 100x left, 1000x right*

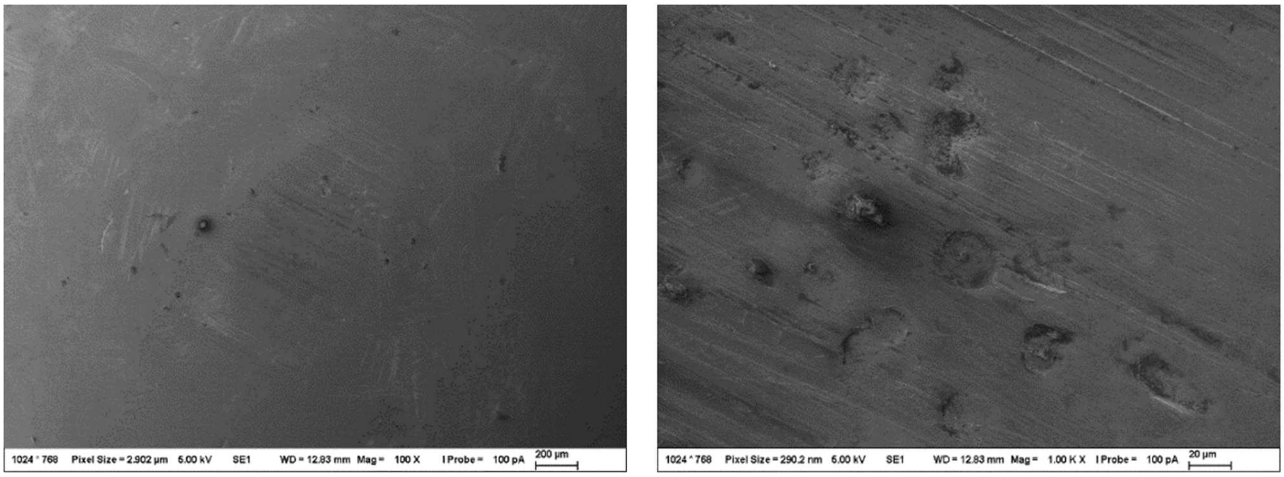

Fig. 23 *Wear of Ti indenter standard, magnification 100x left, 1000x right*

4 Conclusion

The final result of the experiment and its statistical processing is the inference of the influence of the production technology of the used metal component on the above friction and wear parameters. The common phenomenon of all measurements was their course and the resulting graph of the measured friction coefficients, which confirmed the theoretical assumptions. The first phase was the so-called run-in of the sample, when the friction coefficient gradually decreased in the first minutes of measurement. Subsequently, the value of the friction coefficient stabilized in the transition phase. In the third phase, there was an increase in the coefficient of friction due to the initiation of wear processes.

For the purposes of drawing the conclusions of this work, the average values of the coefficient of friction of individual tribological contacts after statistical processing are presented below. Repeated measurements were also included in the data set. For the relevance of the results, the initiation-run-in phase was filtered out.

When testing with liquid, the measured deviations were statistically insignificant due to the technology of the production of the metal component. The 3D printed material showed coefficient of friction values of 0.081; 0.089; 0.102 at loads of 10 N, 15 N and 20 N. With conventionally produced materials, these values were 0.078; 0.082 and 0.098. The values are reflected in the table (Tab. 5).

Tab. 5 *Average coefficients of friction in liquid contact*

Load [N]	COF Ti standard [-]	COF Ti 3D printing [-]	Δ COF [%]
10	0.078	0.081	↑ 3.84
15	0.082	0.089	↑ 8.53
20	0.098	0.102	↑ 4.08
* red numbers represent the increase in COF of the 3D printed sample compared to the standard			

In dry conditions, there were more pronounced deviations due to the technology of metal material production. Depending on the increasing load, the average value of the coefficient of friction increased with 3D printed material from 0.085 to 0.116 to 0.135. For dry conditions and material produced as standard, the values were 0.109; 0.125 and 0.143 at loads of 10, 15 and 20 N. The values are reflected in the table (Tab. 6).

Tab. 6 *Average coefficients of friction in dry contact*

Load [N]	COF Ti standard [-]	COF Ti 3D printing [-]	Δ COF [%]
10	0.109	0.085	↓ 28.24
15	0.125	0.116	↓ 7.76
20	0.143	0.135	↓ 5.93
* green numbers represent the drop in COF of the 3D printed sample compared to the standard			

The width of the wear track was measured in 2 ways. The first method was a profilometer with an induction sensor. The second method was to translate the track with a ruler of the electron microscope elevations. It is possible to see that the values of the width of the measured traces differ from each other depending on the used measurement technique. Higher relevance should be attributed to the method of measuring the track width with the Talysurf profilometer, because the induction probe minimizes the human factor that is introduced when measuring the track width using the translation of the ruler on the zoSEM image.

Based on the above, it can be concluded that the method of manufacturing the metal component of the implant does not have a fundamental influence on the generated friction coefficient and wear parameters of the contact pair of heterogeneous materials from the point of view of tribology. For a detailed explanation of the friction parameters, it is recommended to carry out further analysis of the tested materials, such as metallography or determination of porosity.

Acknowledgement

This research study was supported by the grant "Modern Technologies for the Processing of Advanced Materials Used for Interdisciplinary Applications", FSI-S-22-7957. The Project for the Development of the Organization Military autonomous and robotic assets "DZRO VARoPs" at the Department of Mechanical Engineering, University of Defence.

References

[1] SEDLÁK, J. Moderní technologie výroby implantátu kolenního kloubního se specifickými na tvarové a funkční plochy: Habilitační práce. Brno: Vysoké učení technické v Brně, Fakulta strojního inženýrství, Ústav strojírenské technologie, 2013. 179 s, 9 příloh.

[2] *Stručný nástin historie vývoje aloartroplastiky.* [online]. [vid. 17. února 2012]. Available from: http://ucebnice.euromise.cz/index.php?conn=0&section=biomech&node=node4.

[3] *Totální náhrady lidských kloubů.* [online]. [vid. 4. ledna 2012]. Available from: http://ucebnice.euromise.cz/index.php?conn=0&section=biomech&node=node33.

[4] Informační materiál. Ortopedicko-traumatologické oddělení. Nemocnice Znojmo, p.o. *Totální endoprotéza kolenního kloubu.* [online]. [vid. 25. března 2012]. Available from: http://www.nemzn.cz/vismo/zobraz_dok.asp?id_org=600118&id_ktg=23912&archiv=1&p 1=20092.

[5] VARHANÍK, MATÚŠ. *Využití moderních technologií pro výrobu tvarově složitých ploch* [online]. Brno, 2022 [cit. 2021-09-09]. Available from: https://www.vutbr.cz/studenti/zav-prace/detail/137909. Pojednání. Vysoké učení technické v Brně, Fakulta strojního inženýrství, Ústav strojírenské technologie. Vedoucí práce Josef Sedlák.

[6] DEVLIN, MARK T. Tribology and Wear Modeling and Testing. *Encyclopedia of Materials: Metals and Allloys.* Elsevier, 2022, 589-595. ISBN 9780128197332. Available from: doi:10.1016/B978-0-12-819726-4.00056-9

[7] ZDRAVECNÁ, EVA. Tribológia povrchových vrstiev. Technická univerzita v Košiciach, 2012. ISBN 9788055308852.

[8] DOBROVOLNA, LUCIE, MATUS VARHANIK, JOSEF SEDLAK, ALES POLZER a ZBYNEK STUDENY. The design of a device for testing the tribological properties of knee endoprostheses. *Manufacturing Technology.* ISSN 12132489. Available from: doi:10.21062/mft.2021.064

[9] RUDGE, RAISA E.D., MELISSA J. MOSSELMAN, HEATHER M. SHEWAN, JASON R. STOKES, JOSHUA A. DIJKSMAN a ELKE SCHOLTEN. The impact of tribometer motion and surface roughness on the frictional regimes of model foods. *Food Hydrocolloids* [online]. 2023, 145 [cit. 2023-09-19]. ISSN 0268005X. Available from: doi:10.1016/j.foodhyd.2023.108976

[10] LEKSYCKI, KAMIL; FELDSHTEIN, EUGENE; MARUDA, RADOSŁAW W.; KHANNA, NAVNEET; KRÓLCZYK, GRZEGORZ M. et al. An insight into the effect surface morphology, processing, and lubricating conditions on tribological properties of Ti6Al4V and UHMWPE pairs. Online. *Tribology International.* 2022, roč. 170. ISSN 0301679X. Available from: https://doi.org/10.1016/j.triboint.2022.107504. [cit. 2023-11-25].

[11] ROUDNICKA, MICHAELA; BAYER, FRANTISEK; MICHALCOVA, ALENA; KUBASEK, JIRI; ALZUBI, ENAS GHASSAN HAMED et al. Biomedical titanium alloy prepared by additive manufacturing: Effect of processing on tribology. Online. *Manufacturing Technology.* 2020, roč. 20, č. 6, s. 809-816. ISSN 12132489. Available from https://doi.org/10.21062/mft.2020.112. [cit. 2023-10-16].

[12] ROUDNICKA, MICHAELA; MISURAK, MICHAL; VOJTECH, DALIBOR; KUBASEK, JIRI; ALZUBI, ENAS GHASSAN HAMED et al. Differences in the Response of Additively Manufactured Titanium Alloy to Heat Treatment - Comparison between SLM and EBM: Effect of processing on tribology. Online. *Manufacturing Technology.* 2019, roč. 19, č. 4, s. 668-673. ISSN 12132489. Available from: https://doi.org/10.21062/ujep/353.201

9/a/1213-2489/MT/19/4/668. [cit. 2023-10-16].

[13] HANUSOVÁ, PATRÍCIA; PALČEK, PETER; UHRÍČIK, MILAN; KUBASEK, JIRI; ALZUBI, ENAS GHASSAN HAMED et al. Analysis of the Cause of Titanium Endoprosthesis Failure: Effect of processing on tribology. Online. *Manufacturing Technology*. 2019, roč. 19, č. 5, s. 749-752. ISSN 12132489. Available from: https://doi.org/10.21062/ujep/366.2019/a/1213-2489/MT/19/5/749. [cit. 2023-10-16].

[14] HREN, IRYNA; KUŚMIERCZAK, SYLVIA; HORKÝ, ROMAN; KUBASEK, JIRI; ALZUBI, ENAS GHASSAN HAMED et al. Use of Electron Microscopy in the Analysis of the Influence of Roughness on the Corrosion Behavior of Selected Ti Alloys: Effect of processing on tribology. Online. *Manufacturing Technology*. 2023, roč. 23, č. 2, s. 161-176. ISSN 12132489. Available from: https://doi.org/10.21062/mft.2023.017. [cit. 2023-10-16].

[15] ZHANG, TAO, FENG JIANG, LAN YAN, ZHENGYI JIANG, XIPENG XU a ELKE SCHOLTEN. A novel ultrahigh-speed ball-on-disc tribometer. *Tribology International* [online]. 2021, 157 [cit. 2023-09-19]. ISSN 0301679X. Available from: doi:10.1016/j.triboint.2021.106901

[16] PAWLUS, PAWEL, RAFAL REIZER, LAN YAN, ZHENGYI JIANG, XIPENG XU a ELKE SCHOLTEN. Profilometric measurement of low wear: A review. *Wear* [online]. 2023, 532-533 [cit. 2023-09-19]. ISSN 00431648. Available from: doi:10.1016/j.wear.2023.205102

[17] CAPPELLA, BRUNERO, MANUEL REICHELT, LAN YAN, ZHENGYI JIANG, XIPENG XU a ELKE SCHOLTEN. Origin of lognormal distribution of wear coefficient values: A review. *Tribology International* [online]. 2021, 164 [cit. 2023-09-19]. ISSN 0301679X. Available from: doi:10.1016/j.triboint.2021.107207